

Published in final edited form as:

J Biochem Mol Biol. 2005 March 31; 38(2): 243–247.

Secondary Structure,¹H, ¹³C and ¹⁵N Resonance Assignments and Molecular Interactions of the Dishevelled DIX Domain

Daniel G. S. Capelluto[†] and Michael Overduin^{‡,*}

[†]Department of Pharmacology, University of Colorado Health Sciences Center at Fitzsimons, Mail Stop F8303, Aurora, Colorado, USA, 80045

[‡]CR UK Institute for Cancer Studies, School of Medicine, University of Birmingham, Birmingham B15 2TT, United Kingdom

Abstract

Dishevelled (Dvl) is a positive regulator of the canonical Wnt signaling pathway, which regulates the levels of β -catenin. The β -catenin oncoprotein depends upon the association of Dvl and Axin proteins through their DIX domains, and its accumulation directs the expression of specific developmental-related genes at the nucleus. Here, the ¹H, ¹³C, and ¹⁵N resonances of the human Dishevelled 2 DIX domain are assigned using heteronuclear nuclear magnetic resonance (NMR) spectroscopy. In addition, helical and extended elements are identified based on the NMR data. The results establish a structural context for characterizing the actin and phospholipid interactions and binding sites of this novel domain, and provide insights into its role in protein localization to stress fibers and cytoplasmic vesicles during Wnt signaling.

Keywords

Dishevelled; DIX domain; Resonance assignments

Introduction

The Wnt signaling pathway is crucial in cell differentiation and proliferation of embryonic and adult tissues, and its disruption leads to human tumors including colorectal cancer (Nelson and Nusse, 2004). Signaling is initiated by secreted Wnt glycoproteins, which bind to seven transmembrane Frizzled receptors and the low-density receptor-related lipoproteins at the cell surface. Downstream events include positive and negative regulation of β -catenin levels by two DIX domain-containing proteins, Dishevelled (Dvl) and Axin, respectively. In unstimulated cells, β -catenin is targeted for destruction in the ubiquitin-proteasome pathway by a protein complex that includes the Axin protein, a putative tumor suppressor (Satoh *et al.*, 2000). Under specific Wnt stimulation, Dvl binds to Axin and disassembles the β -catenin destruction complex. Thus, Dvl boosts the intracellular levels of β -catenin, which translocates to the nucleus where it binds to transcription factors leading to changes in gene expression.

The DIX domain is a 85-residue conserved module found in a family of seven human signaling proteins. Dvl and Axin represent the two major subtypes of DIX domain-containing proteins, and their homo and hetero oligomerization is mediated by their DIX domains (Kishida *et al.*, 1999). A third subtype of a DIX-related protein, the coiled-coil-

* To whom correspondence should be addressed. Tel: 44-121-414-3802; Fax: 44-121-414-4486, E-mail: m.overduin@bham.ac.uk.

DIX1, has been recently shown to positively regulate Wnt signaling by hetero oligomerization with Dvl and Axin (Shiomi *et al.*, 2003). The DIX domain interacts with actin stress fibers and vesicular membranes, partitioning Dvl between these two pools and segregating the proteins to distinct pathways (Capelluto *et al.*, 2002). In addition to the N-terminal DIX domain, the three mammalian Dvl proteins (Dvl1, Dvl2, and Dvl3) contain DEP and PDZ domains in their sequences of approximately 700 residues, and these modules are generally thought to mediate membrane and protein interactions, respectively (Wharton, 2003). The involvement of Dvl in the Wnt pathway requires the integrity of its DIX and PDZ domains while its DEP domain may coordinate planar cell polarity through the Jun N-terminal kinase cascade (Wharton, 2003).

In order to obtain further insights into structure-function relationships of Dvl, we carried out NMR studies of its conserved DIX domain. Here we report the NMR characterization of the homodimeric DIX domain of the Dishevelled 2 (Dvl2) protein.

Materials and Methods

The DIX domain of human Dvl2 (residues 10-94) was overexpressed in *E. coli* BL21(DE3)pLysS strain (Novagen, Madison, USA) as a glutathione S-transferase (GST) fusion protein. Unlabeled protein was purified from cells grown at 30°C in Luria-Bertani broth. Uniformly ^{15}N and $^{13}\text{C}/^{15}\text{N}$ labeled DIX was produced in M9 minimal media supplemented with $^{15}\text{NH}_4\text{Cl}$ and $^{13}\text{C}_6$ -glucose (Cambridge Isotope Laboratories). Harvested cells were disrupted by sonication. The GST- fusion protein was immobilized and purified on Glutathione Sepharose 4B beads (Amersham, Arlington Heights, USA). Dvl2 DIX was eluted by cleavage with thrombin (Sigma Chemical Co, St. Louis, USA), concentrated in the presence of 7 mM perdeuterated dodecylphosphocholine (DPC-d₃₈) (Cambridge Isotope Laboratories), and its purity was verified by SDS-PAGE. The dimeric state of the DIX domain was evidenced from its diffusion coefficient determined by the pulse field gradient experiments and from SDS PAGE and bis(sulfosuccinimidyl) suberate crosslinking experiments (Capelluto *et al.*, 2002).

NMR samples contained 0.2-1 mM of the DIX domain, 90% $\text{H}_2\text{O}/10\%$ $^2\text{H}_2\text{O}$ or 99.9% $^2\text{H}_2\text{O}$, 20 mM Tris-d₁₁ (pH 6.5) buffer, 600 mM DPC-d₃₈, 1 mM dithiothreitol-d₁₀, 1 mM NaN_3 and 50 mM 4-amidinophenylmethane sulfonyl fluoride. NMR experiments were performed at 303 K on Varian INOVA 600 and 500 MHz spectrometers equipped with triple resonance shielded probes with z-axis pulse field gradients. Spin system and sequential assignments were made from ^1H , ^{15}N -HSQC, CBCA(CO)NNH, HNCACB, HNCO, HNHA, H(CCO)NH TOCSY, C(CO)NH TOCSY, ^{15}N -edited TOCSY, ^{15}N -edited HSQC-NOESY and HSQC-NOESY-HSQC experiments ($\tau_{\text{mix}}=50$ and 135 ms) (Grzesiek *et al.*, 1993; Kay *et al.*, 1993; Muhandiram and Kay, 1994) (Fig. 1). Asn and Gln side chain ^1H and ^{15}N resonances were assigned using 3D ^{15}N -edited NOESY and 3D CBCA(CO)NNH spectra. The secondary structure elements were identified from $J_{\text{HNH}\alpha}$ coupling constants derived from HNHA (Vuister and Bax, 1993) and HMQC-J spectra, medium and sequential NOEs patterns, and $^1\text{H}_\alpha$, $^{13}\text{C}_\alpha$, $^{13}\text{C}_\beta$, and ^{13}CO chemical shifts (Wishart and Sykes, 1994). Titrations of G-actin (Cytoskeleton) into the ^{15}N -labeled DIX domain were analyzed by HSQC experiments. Spectra were processed with NMRPipe (Delaglio *et al.*, 1995) and analyzed using PIPP (Garrett *et al.*, 1991), nmrDraw and in-house software programs (<http://biomol.uchsc.edu>).

Results and Discussion

The $^1\text{H}_\text{N}$ and ^{15}N resonances of all 80 backbone amides (excluding the five Pro residues) and ^{13}C resonances of 77 of the 85 backbone carbonyls of the human Dvl2 DIX were

assigned. The majority of the spin systems of the Dvl2 DIX domain were identified by the analysis of the H(CCO)NH TOCSY and C(CO)NH TOCSY experiments. In total, 100% of H α , 99% of H β , H γ , H δ and H ϵ , 98% of C α , 99% of C β and 52% of C γ , C δ , C ϵ and C η resonances were assigned. All the aromatic side chain protons of five Phe, three Tyr, one Trp and three His and the ^1H and ^{15}N resonances for the NH $_2$ side chains of 2 Asn and 2 Gln were assigned completely. No assignments were made for the guanidino moiety of Arg and the side chain NH $_3^+$ of Lys. The chemical shift values of the ^1H , ^{15}N and ^{13}C resonances are represented in Table 1. A typical ^1H ^{15}N HSQC spectrum is shown in Fig. 2, where the backbone NHs are labeled for its corresponding amino acid. Chemical shift index analysis of the H α , $^{13}\text{C}\alpha$ and $^{13}\text{C}\text{O}$ resonance assignments together with NOEs patterns in 3D ^{15}N -edited NOESY and coupling constants estimated from the HNHA experiment indicated the presence of two α -helices (residues Ala35-Gln48 and Ala51-Tyr55), as well as helical and extended elements (Asn82-Leu89 and Val29-Ile31, respectively) (Fig. 3).

The ability of the DIX domain to interact with membranes was studied using DPC micelles. A number of structural determinations of membrane proteins bound to micelles have indicated that valuable structural information can be obtained from NMR studies of such systems (Henry and Sykes, 1994). The DIX domain mediates Dvl2 localization to vesicular membranes, where activates canonical Wnt signaling by stabilization of β -catenin (Capelluto *et al.*, 2002). HSQC spectra of the DIX domain were collected during stepwise of DPC micelle addition. Several chemical shifts changes in the backbone amides of DIX were detected and plotted as a histogram (Fig. 4A). The data indicates that a short stretch between the last two helical elements in the Dvl2 DIX domain is a putative membrane recognition motif.

The DIX domain has also been shown to bind to actin stress fibers, where it may activate non-canonical Wnt signaling (Capelluto *et al.*, 2002). Thus, we mapped the DIX domain actin-binding site using a similar approach as described for DPC binding. The residues interacting with the actin are evident from the chemical shift perturbations (Fig. 4B). This actin-binding site is localized between the second helix and the DPC binding site, as identified by chemical shift changes induced by stepwise addition of G-actin (Fig. 4B). The actin binding motif of DIX is similar to those described for MARCKS and actobindin proteins (Maciver, 1995). As shown in Fig. 4C, the amino acid sequence alignment of DIX domain-containing proteins indicates that both DPC and actin-interacting residues are predominantly conserved among the DIX proteins. This suggests that the actin and micelle interactions may be extended to other members of the family of DIX domain-containing proteins. Thus, the information provided here provides a structural basis for understanding the ligand interactions and molecular function of the DIX domain.

Acknowledgments

We thank D. Jones for discussions, R. Muhandiram and L. E. Kay for NMR pulse sequences. The NMR Center is supported by the University of Colorado Cancer Center Core. This work was supported by the National Institutes of Health, Royal Society and BBSRC (M.O.) and the Cancer League of Colorado (D.G.S.C.).

References

- Capelluto DG, Kutateladze TG, Habas R, Finkielstein CV, He X, Overduin M. The DIX domain targets dishevelled to actin stress fibres and vesicular membranes. *Nature*. 2002; 419:726–729. [PubMed: 12384700]
- Delaglio F, Grzesiek S, Vuister GW, Zhu G, Pfeifer J, Bax A. NMRpipe—a multidimensional spectral processing system based on Unix pipes. *J. Biomol. NMR*. 1995; 6:277–293. [PubMed: 8520220]

- Garrett DS, Powers R, Gronenborn AM, Clore GM. A common-sense approach to peak picking in 2-dimensional, 3-dimensional, and 4-dimensional spectra using automatic computer-analysis of contour diagrams. *J. Magn. Reson.* 1991; 95:214–220.
- Grzesiek S, Anglister J, Bax A. Correlation of backbone amide and aliphatic side-chain resonances in C-13/N-15-enriched proteins by isotropic mixing of C-13 magnetization. *J. Magn. Reson.* 1993; 101:114–119.
- Henry GD, Sykes BD. Methods to study membrane protein structure in solution. *Methods Enzymol.* 1994; 239:515–535. [PubMed: 7830597]
- Kay LE, Xu GY, Singer AU, Muhandiram DR, Formankay JD. A gradient-enhanced HCCH TOCSY experiment for recording side-chain H-1 and C-13 correlations in H₂O samples of proteins. *J. Magn. Reson.* 1993; 101:333–337.
- Kishida S, Yamamoto H, Hino S, Ikeda S, Kishida M, Kikuchi A. DIX domains of Dvl and Axin are necessary for protein interactions and their ability to regulate beta-catenin stability. *Mol. Cell. Biol.* 1999; 19:4414–4422. [PubMed: 10330181]
- Maciver, SK. Microfilament organization and actin binding proteins. In: Hesketh, JE.; Pryme, IF., editors. *Treatise on the Cytoskeleton; Structure and Assembly.* JAI press; Greenwich, United Kingdom: 1995. p. 1-45.
- Muhandiram DR, Kay LE. Gradient-enhanced triple-resonance 3-dimensional NMR experiments with improved sensitivity. *J. Magn. Reson.* 1994; 103:203–216.
- Nelson WJ, Nusse R. Convergence of Wnt, beta-catenin, and cadherin pathways. *Science.* 2004; 303:1483–1487. [PubMed: 15001769]
- Satoh S, Daigo Y, Furukawa Y, Kato T, Miwa N, Nishiwaki T, Kawasoe T, Ishiguro H, Fujita M, Tokino T, Sasaki Y, Imaoka S, Murata M, Shimano T, Yamaoka Y, Nakamura Y. AXIN1 mutations in hepatocellular carcinomas, and growth suppression in cancer cells by virus-mediated transfer of AXIN1. *Nat. Genet.* 2000; 24:245–250. [PubMed: 10700176]
- Shiomi K, Uchida H, Keino-Masu K, Masu M. Ccd1, a novel protein with a DIX domain, is a positive regulator in the Wnt signaling during zebrafish neural patterning. *Curr. Biol.* 2003; 13:73–77. [PubMed: 12526749]
- Vuister GW, Bax A. Quantitative J correlation - a new approach for measuring homonuclear 3-bond J(H(N)H(alpha)) coupling-constants in N-15-enriched proteins. *J. Am. Chem. Soc.* 1993; 115:7772–7777.
- Wharton KA Jr. Runnin' with the Dvl: proteins that associate with Dsh/Dvl and their significance to Wnt signal transduction. *Dev. Biol.* 2003; 253:1–17. [PubMed: 12490194]
- Wishart DS, Sykes BD. The 13C chemical-shift index: a simple method for the identification of protein secondary structure using 13C chemical-shift data. *J. Biomol. NMR.* 1994; 4:171–180. [PubMed: 8019132]

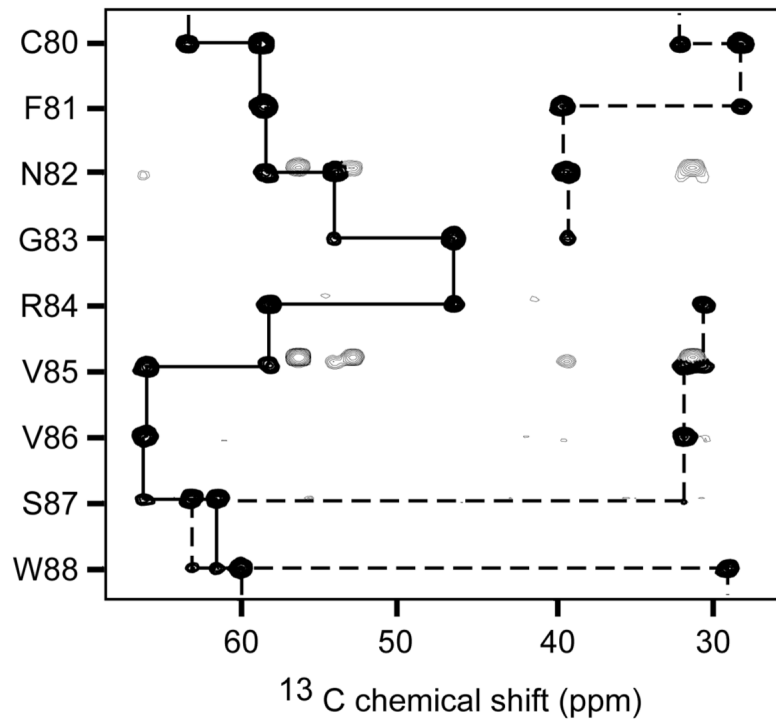


Fig. 1. Representative strips from the HNCACB spectrum of Dvl2 DIX domain (1 mM) collected at 303 K showing sequential connectivities for $\text{C}\alpha$ (solid line) and $\text{C}\beta$ (dotted line) resonances of residues Cys80-Trp88 of the domain.

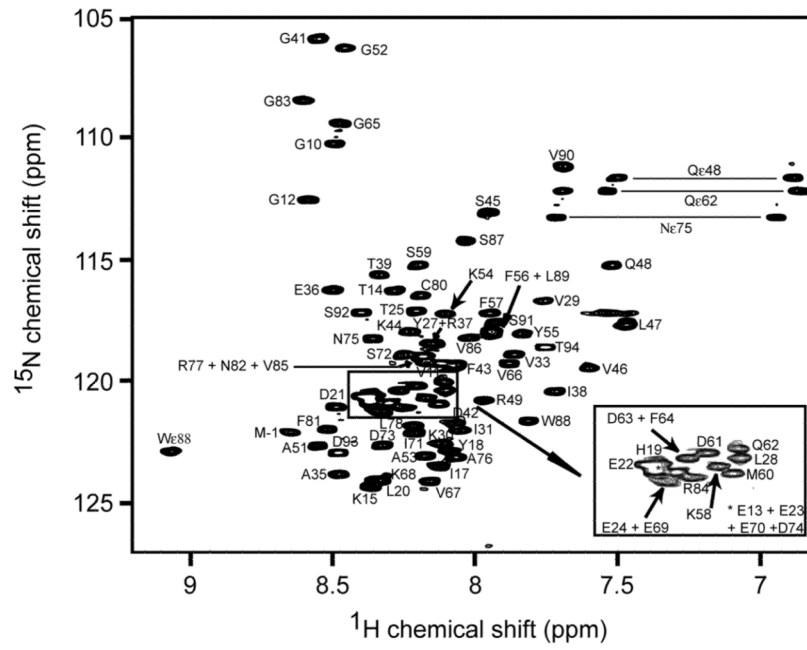


Fig. 2. Two dimensional ^1H ^{15}N HSQC spectrum of $200\ \mu\text{M}$ ^{15}N -labeled Dv12 DIX domain acquired at 600 MHz. Selected peaks are labeled with the corresponding residue numbers.

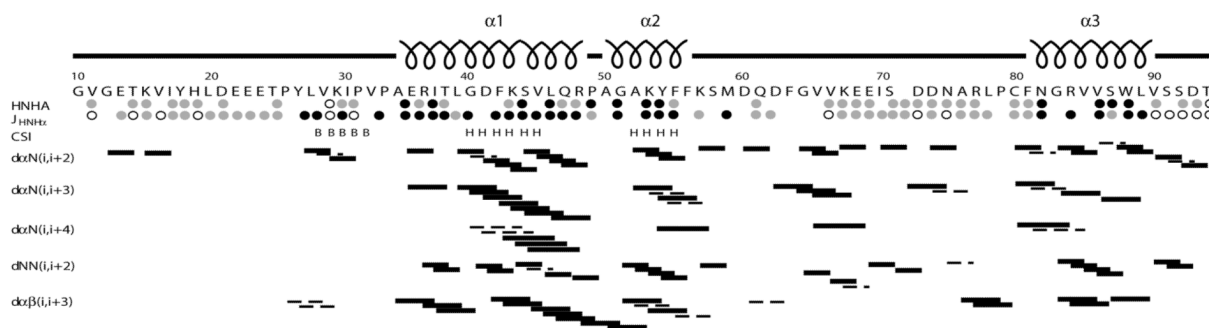


Fig. 3. Predicted secondary structure of the Dvl2 DIX domain. The predictions are based on consensus chemical shift indices (CSI's), coupling constants, and local NOEs. The CSI predictions of helical (H) and extended (B) conformations were based on each residues $^1\text{H}_\alpha$, $^{13}\text{C}_\alpha$, $^{13}\text{C}_\beta$, and $^{13}\text{C}'$ chemical shifts. The $J_{\text{HNH}\alpha}$ coupling constants under 6 Hz (black circle), over 8 Hz (open circle), and between 6 and 8 Hz (grey circles) are consistent with helical, extended, and indeterminate secondary structure, respectively, and were estimated from HNHA and HMQC-J spectra. The NOE connectivities provide distances (d) between the HN (N), H_a (a), and H_b (b) resonances of residues that are $i = 2, 3,$ or 4 positions apart, and are indicated as solid and dashed lines depending on whether they are resolved or partially overlapped, respectively, in NOESY spectra collected with NOE mixing times of 50 and 135 ms.

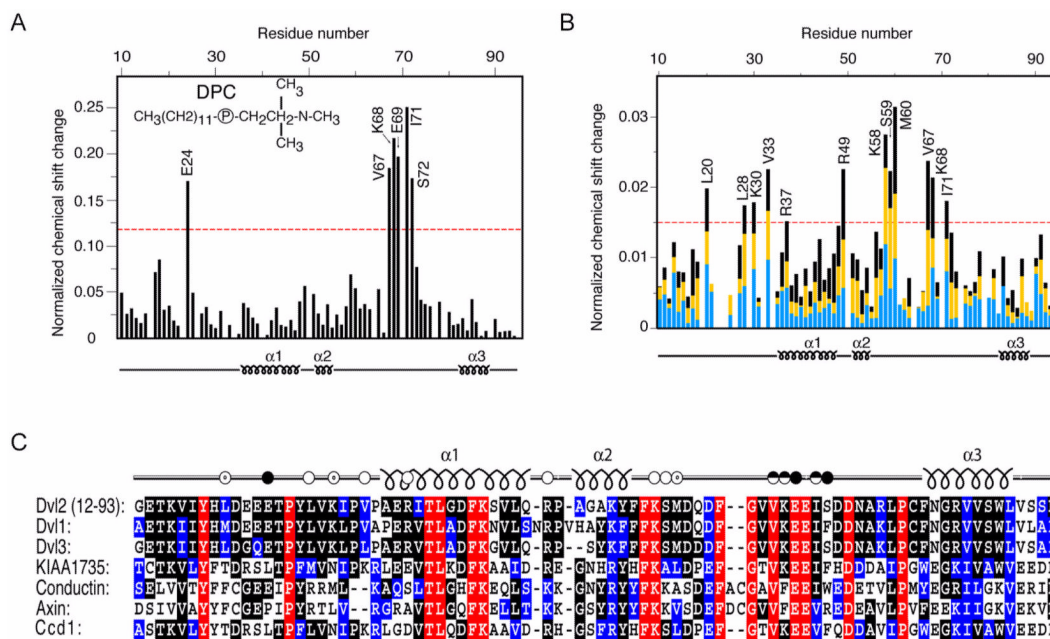


Fig. 4. Identification of ligand-interacting residues of the DIX domain by HSQC experiments. (A) The histogram displays the normalized chemical shift difference for each residues amide group of ^{15}N -labeled Dvl2 DIX domain (100 μM) caused by increasing the d_{38} -DPC concentration from 10 to 400 mM. (B) Histogram showing the progressive changes in chemical shifts of DIX domain (100 μM) residues following actin addition. Blue, yellow and black bars represent reductions after addition of 200, 300 and 400 μM G-actin, respectively. The ^1H , ^{15}N chemical shifts were normalized as $([(\Delta\delta_{\text{H}})^2 + (\Delta\delta_{\text{N}}/5)^2]/2)^{0.5}$, where δ is chemical shift in parts per million (ppm). Labeled residues exhibit changes that exceed the red line, which represents 50% of the largest change. (C) The amino acid sequences of the DIX domains from human Dvl1 homologs, KIAA1735, Conductin and Axin and zebrafish Ccd1 are aligned. Identical, highly conserved and similar residues are shown in red, black and blue, respectively. The Dvl2 residues that are involved in actin and DPC micelle binding are shown with unfilled and filled dots, respectively.

Table 1

Chemical shifts of $^1\text{H}_\text{N}$, ^{15}N , ^{13}CO , ^{13}Ca and $^{13}\text{C}\beta$ of the Dvl2 DIX domain. All chemical shifts were referenced relative to the frequency of the methyl proton resonance of DSS. ND: not determined

Residue	HN	N	CO	Ca	C β
10GLY	8.45	109.92	173.96	45.34	
11VAL	8.09	119.08	176.61	62.58	32.67
12GLY	8.58	112.37	176.06	45.41	
13GLU	8.29	120.81	174.08	56.54	30.46
14THR	8.24	116.15	174.12	62.35	69.77
15LYS	8.34	124.17	175.90	56.22	33.25
16VAL	8.18	121.42	175.42	62.37	32.83
17ILE	8.13	123.73	175.12	60.84	38.77
18TYR	8.05	123.17	174.68	57.43	39.36
19HIS	8.31	120.34	173.80	55.28	29.75
20LEU	8.32	123.83	176.47	55.11	42.58
21ASP	8.44	120.94	ND	54.45	41.13
22GLU	8.35	120.91	176.42	56.86	30.35
23GLU	8.35	121.00	176.21	56.60	30.43
24GLU	8.36	122.10	176.26	56.52	30.43
25THR	8.20	117.26	ND	60.06	69.50
26PRO			176.46	63.40	32.05
27TYR	8.16	118.51	175.64	58.65	38.53
28LEU	8.10	119.94	176.61	56.05	42.48
29VAL	7.74	116.73	175.06	62.02	32.99
30LYS	8.10	122.66	175.61	55.67	33.10
31ILE	8.05	122.10	ND	58.48	38.59
32PRO			175.13	63.07	31.31
33VAL	7.84	118.88	ND	59.59	33.07
34PRO			175.42	62.94	31.73
35ALA	8.45	123.75	177.99	53.62	19.27
36GLU	8.46	116.36	176.20	56.89	30.11
37ARG	8.12	118.5	175.53	55.94	30.69

Residue	HN	N	CO	C α	C β
38ILE	7.71	120.38	174.55	60.66	38.79
39THR	8.30	115.64	175.07	60.07	71.76
40LEU	9.04	122.74	178.80	57.49	41.91
41GLY	8.51	105.80	175.86	46.75	
42ASP	8.03	121.59	177.77	56.43	40.91
43PHE	8.05	119.36	176.56	60.11	39.14
44LYS	8.18	117.97	177.97	59.96	32.29
45SER	7.92	113.00	176.28	60.98	62.97
46VAL	7.56	119.29	176.12	64.29	31.76
47LEU	7.44	117.68	176.35	55.68	41.85
48GLN	7.50	115.35	175.68	55.70	29.51
49ARG	7.98	120.95	ND	55.25	29.85
50PRO			177.02	64.07	31.82
51ALA	8.52	122.85	178.82	53.76	18.91
52GLY	8.43	106.33	174.49	45.93	
53ALA	8.15	122.97	177.99	53.77	19.06
54LYS	8.08	117.33	176.84	58.01	32.58
55TYR	7.80	118.00	176.01	59.24	38.73
56PHE	7.92	117.78	175.39	59.29	39.69
57PHE	7.90	116.99	175.79	58.13	39.34
58LYS	8.15	121.00	176.78	57.15	32.91
59SER	8.22	115.51	174.68	58.95	63.61
60MET	8.16	121.12	175.75	55.88	32.79
61ASP	8.17	120.32	176.15	54.65	41.13
62GLN	8.10	119.47	176.06	56.00	29.59
63ASP	8.23	120.44	175.26	54.24	41.19
64PHE	8.24	120.50	176.17	58.37	39.24
65GLY	8.40	109.60	173.97	45.70	
66VAL	7.84	119.25	176.02	62.65	32.74
67VAL	8.16	123.89	175.83	62.55	32.61
68LYS	8.36	125.37	176.13	56.43	33.19

Residue	HN	N	CO	Cα	Cβ
69GLU	8.38	122.40	ND	ND	ND
70GLU	8.35	120.91	176.18	56.22	30.30
71ILE	8.19	121.90	175.96	60.97	38.60
72SER	8.33	119.79	174.15	58.08	64.09
73ASP	8.35	122.91	176.21	54.35	41.31
74ASP	8.34	121.00	176.47	54.96	40.94
75ASN	8.32	118.40	175.12	53.68	38.97
76ALA	8.05	123.17	177.24	52.67	19.18
77ARG	8.18	119.13	175.90	56.20	31.14
78LEU	8.19	121.73	ND	53.20	42.01
79PRO			175.82	63.07	31.87
80CYS	8.18	116.54	174.32	58.47	28.08
81PHE	8.51	121.87	175.03	58.18	39.34
82ASN	8.17	118.86	175.65	53.78	39.12
83GLY	8.55	108.31	175.17	46.29	
84ARG	8.22	121.00	177.94	58.18	30.43
85VAL	8.16	119.14	176.96	63.43	31.94
86VAL	8.00	118.10	177.05	ND	31.89
87SER	8.00	114.03	175.86	61.32	62.93
88TRP	7.78	121.52	177.14	59.84	28.94
89LEU	7.91	117.70	176.93	57.03	43.00
90VAL	7.65	110.88	175.71	61.50	32.49
91SER	7.89	117.47	174.25	58.38	63.81
92SER	8.37	117.03	174.14	58.18	64.05
93ASP	8.45	122.88	175.43	54.55	41.16
94THR	7.72	118.49	ND	63.12	70.75